ELSEVIER

Biophysical Chemistry 68 (1997) 83–93

Biophysical Chemistry

Intermediate filament structure: hard α-keratin

L.N. Jones [a,*], M. Simon [b], N.R. Watts [c], F.P. Booy [c], A.C. Steven [c], D.A.D. Parry [d]

[a] *CSIRO Division of Wool Technology, P.O. Box 21, Belmont, Vic. 3216, Australia*
[b] *Brookhaven National Laboratory, Upton, NY 11973, USA*
[c] *Laboratory of Structural Biology Research, National Institute of Arthritis Musculoskeletal and Skin Diseases, 6 Center Drive MSC 2717, National Institutes of Health, Bethesda, MD 20892-0001, USA*
[d] *Department of Physics, Massey University, Private Bag 11-222, Palmerston North, New Zealand*

Received 19 November 1996; accepted 13 January 1997

Abstract

Structurally there are four classes of intermediate filaments (IF) with distinct but closely related axial organisations. One of these, hard α-keratin IF, has been studied to clarify several apparently exceptional features which include the number of molecules in the IF cross-section and the mode by which the axial organisation of its constituent molecules is stabilised. Using the dark-field mode of the STEM at the Brookhaven National Laboratory (USA) mass measurements were obtained from unstained IF isolated from hair keratin. The data thus obtained show that the number of chains in cross-section is about 30 (±3: standard deviation) and is very similar to the numbers determined in previous STEM experiments for the dominant filament type in other classes of IF (about 32). Furthermore, re-analysis of the low-angle equatorial X-ray diffraction pattern reveals, in contrast to earlier work, solutions that are compatible with the number of chains in cross-section indicated by the STEM data. The absence of the head-to-tail overlap between parallel molecules characteristic of most IF may be compensated in hard α-keratin by a network of intermolecular disulfide bonds. It is concluded that native IF of hard α-keratin and desmin/vimentin —and probably many other kinds of IF as well— contain about 32 chains in cross-section, and that the axial structures of these various kinds of IF differ in small but significant ways, while generally observing the same basic modes of aggregation. © 1997 Elsevier Science B.V.

Keywords: Intermediate filament; Wool; α-Keratin; Disulfide bonds; Mass measurements; X-ray diffraction

1. Introduction

At the ultrastructural level hard α-keratin from hair, nails, claws, beaks, quills, hooves, baleen and horns consists of intermediate filaments (IF) with diameters of about 7–8 nm embedded in an osmiophilic protein matrix [1] (Fig. 1). Characterisation of the constituent proteins has revealed four major classes, based in large part on their relative cysteine residue contents: the low-sulfur proteins, the high-sulphur proteins, the ultra high-sulfur proteins and the high-tyrosine proteins. The low-sulfur proteins contain about 50% α-helix but there is no measurable α-helix in any of the other classes of proteins. Since an oriented α-type X-ray diffraction pattern could be obtained from hard α-keratin it was believed (and subsequently proved) that the low-sulfur

* Corresponding author.

PII S0301-4622(97)00013-6

proteins constituted the bulk of the IF and that the remaining proteins formed the highly disulfide-bonded matrix. Chemical characterisation of isolated hard α-keratin IF confirmed that the composition matched that of the low-sulfur proteins [2]. In some α-keratins there is an additional level of structure. In the case of a crimped fine wool fibre, for example, the concave and convex sides of the fibre are formed from columns of cells that constitute the so-called paracortex and orthocortex respectively. Chemically and structurally these differ significantly: in the paracortex the IF are arranged in a quasi-hexagonal array, whereas in the orthocortex they are arranged in swirls [3] (Fig. 1). The paracortex also has a higher cysteine content than the orthocortex, a lower content of the high-tyrosine proteins and has more matrix overall [3–5].

Much is known of the molecular structure of hard α-keratin and of the manner in which the molecules aggregate to form the IF. Eight low-sulphur proteins (8a, 8b, 8c-1, 8c-2, 5, 7a, 7b and 7c) have been identified as components of the IF [6] and, on the basis of sequence homology, these have been classified as either Type I (8a, 8b, 8c-1, 8c-2) or Type II chains (5, 7a, 7b, 7c). There is very high sequence identity within each family. The N- and C-terminal domains of each hard α-keratin chain are rich in cysteine residues whereas the intervening region contains few such residues. This region, however, does have a heptad substructure of the form $(a–b–c–d–e–f–g)_n$, with positions a and d commonly occupied by apolar residues [7]. This motif is characteristic of a coiled-coil conformation in which right-handed α-helices coil around one another in a left-handed manner to form a rod-like structure, in this case of predicted total length 46 nm. Within this rod there are three breaks in the heptad continuity, designated by links L1, L12 and L2. These connect coiled-coil segments 1A to 1B, 1B to 2A, and 2A to 2B respectively (Fig. 2). There is an additional phasing discontinuity, known as a 'stutter' (the deletion of three residues from an otherwise continuous heptad substructure), located close to the centre of segment 2B (Fig. 2). This stutter is believed to represent a point at which the coiled-coil undergoes a degree of local unwinding [8]. A number of previous studies have shown that the hard α-keratin molecule is an obligate heterodimer containing a Type I and a Type II chain, where these chains are arranged parallel to one another and in axial register [9–11]. At the N-terminal end of segment 1A and the C-terminal end of segment 2B there are regions of sequence which are highly conserved across all IF types irre-

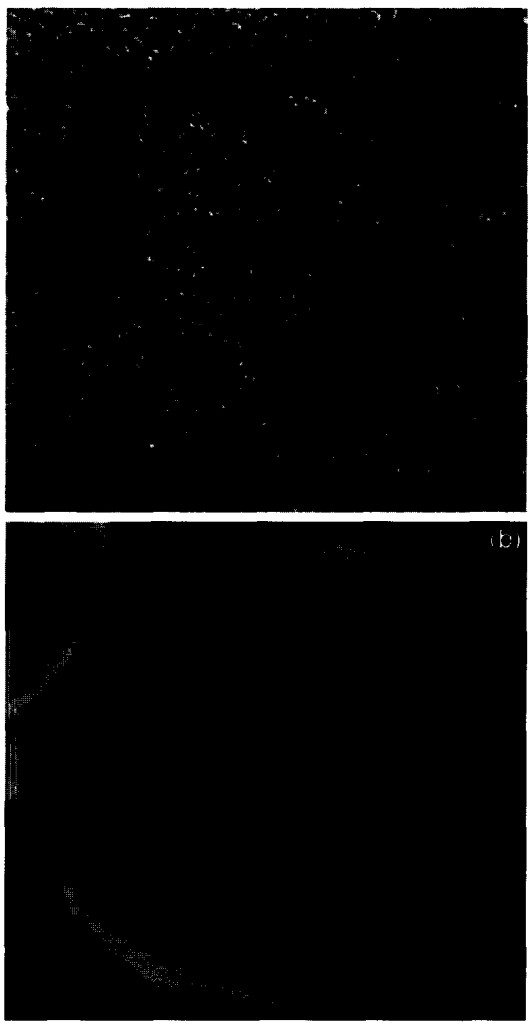

Fig. 1. (a) Human hair keratin IF in cross-section after staining with osmium tetroxide, uranyl acetate and lead citrate. The hair fibres were reduced in thioglycollic acid prior to staining. Under these conditions of staining IF show an annular (ring-core) substructure. The interfilamentous matrix is densely stained. Magnification about 240,000×. (b) Merino wool fibre cross-section stained with Eosin-Y and observed in dark field using a UV light source. The ortho/para-cortex is clearly differentiated and strong fluorescence can be seen in the outer cuticle cells, the cell membrane complex and the nuclear remnants (courtesy of Ms C Coombs, CSIRO Division of Wool Technology).

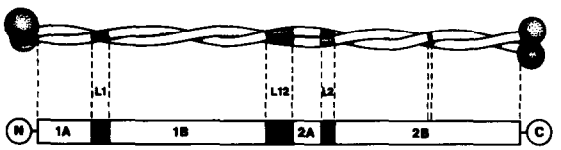

Fig. 2. The N- and C-terminal domains of a hard α-keratin heterodimer contain many cysteine residues involved in the formation of disulfide bonds with other IF molecules and matrix proteins. Between the terminal domains lies a region which forms a left-handed coiled-coil rod (segments 1A, 1B, 2A, 2B) with a total length of about 46 nm. Breaks in the coiled-coil rod occur at links L1, L12 and L2 and there is a 'stutter' in the heptad phasing close to the centre of segment 2B.

spective of origin. In the case of epidermal keratin, vimentin, neurofilaments and lamin there is evidence that these sequences are axially aligned, and give rise to a head-to-tail overlap between parallel molecules in the IF. This overlap is thought to provide a key interaction in stabilising the molecular assembly [1]. Evidence will be provided in this contribution that this interaction appears to be absent in hard α-keratins.

Another feature of particular interest in the rod domain is the highly regular linear disposition of acidic and basic residues. This arrangement occurs in both segment 1B (period 9.55 residues) and segment 2 (= 2A + L2 + 2B) (period 9.85 residues). Furthermore, in each of these long coiled-coil regions the periods in the acidic and basic residues are out of phase with one another. Such a regularity strongly indicates a likely method by which the molecules will aggregate i.e. through the maximisation of intermolecular ionic interactions [9,12–14]. Five potential models were proposed by Crewther et al. [15] though only those three associated with an antiparallel aggregation of molecules were believed likely. Subsequent crosslinking studies on epidermal keratin [16,17] and vimentin [18] have confirmed these modes of aggregation and allowed the axially projected lengths of the links and the precise axial staggers between the coiled-coil segments to be refined using a least squares analysis [16–18]. In the case of hard α-keratin, such crosslinking techniques have not proved possible and instead a different approach has been used (see below).

The modes of molecular aggregation seem to be essentially common to epidermal keratin and vimentin IF, although the exact values of the relative axial staggers between coiled-coil segments and the lengths of the links differ between the two systems [16–18]. In these IF and in neurofilaments [19] the number of chains in cross-section is thought to be about 32 with axial stabilisation being achieved in part through a head-to-tail overlap between conserved regions of sequence at either end of the rod domain. In hard α-keratin filaments, on the other hand, prior evidence —primarily the effective diameter of the filament as deduced from low-angle X-ray diffraction patterns [20]— has been taken to suggest that the number of chains in cross-section may be significantly less, perhaps as low as 23 [21]. Data from β-keratin would also seem to support this possibility [22]. To address this apparent anomaly we have used the Brookhaven scanning transmission electron microscope (STEM) to perform measurements of mass-per-unit-length [23] of hard α-keratin filaments isolated from rat vibrissae. Taking into account the axial repeat of 47 nm [24,25] and the molecular weights of the chains the results show that the number of chains in cross-section is indistinguishable from those in epidermal keratin and vimentin IF (i.e. about 32). In view of this finding we propose that the head-to-tail molecular overlap is indeed absent in hard α-keratin filaments; instead, the stability of these filaments can be accounted for in terms of a network of intermolecular disulfide bonds.

2. Materials and methods

2.1. Isolation of hair keratin intermediate filaments

Vibrissae were plucked from freshly killed albino rats or freshly plucked human head hairs and placed in phosphate buffered saline (PBS) solution previously cooled in ice. Vibrissae follicles were examined under a binocular microscope and those in the anagen phase selected for isolation of presumptive hair shaft (PHS) cells. Cells comprising the inner root sheath and outer root sheath were carefully removed by microdissection in PBS solution. The PHS was separated from the vibrissae and further dissected to isolate a tissue piece from the lower bulb region (first one-third section). This tissue was

briefly immersed in sterile distilled water and transferred to a sterile Eppendorf tube containing 100 μl of sterile distilled water. About 30–40 tissue pieces were collected in like manner and tissue pieces were left to swell in distilled water. A sterile glass rod was subsequently used to break up the tissue pieces gently. Dispersions of IF were liberated into the distilled water after cell lysis. These preparations were centrifuged at 3000 *g* for 30 min at 4°C. The supernatant containing purified IF was then transferred to a sterile Eppendorf tube for analysis and ultrastructural studies. Isolated IF were stored on ice or at 4°C in preparation for transport or other studies. The method described here is a refinement of that initially proposed by Jones and Pope [26].

2.2. STEM measurements

Freshly prepared filaments (Section 2.1) were visualized at the STEM facility at the Brookhaven National Laboratory (Upton, NY, USA), as described previously [27–29]. In brief, specimens were absorbed without further dilution to thin carbon films using the 'wet film' method (see [28]); washed ten times by serial transfer on to drops of 20 mM ammonium acetate to remove non-volatile salts; blotted to a thin film; quick-frozen by immersion into liquid-N_2 slush; and allowed to freeze-dry at a constant sublimation rate over 6–8 h. Tobacco mosaic virus was preadsorbed to the substrate to serve as an internal mass standard (131.4 kDa nm^{-1}). These unstained specimens were imaged in the STEM dark-field mode, with direct recording of digital micrographs of 512×512 pixels, which covered fields of $(1.024\ \mu m)^2$ in the data analyzed. Mass measurements [23] were performed by interactive analysis of displayed micrographs, using the PIC image processing programs [30], running on an Alpha 3000-900 work-station (Digital Equipment Corporation).

2.3. STEM analysis

Over 300 mass measurements were made of hard α-keratin IF isolated from rat vibrissae (Fig. 3). The distribution of mass-per-unit-length measurements (Fig. 4) is unimodal like the distribution recorded for native desmin/vimentin copolymer filaments isolated from BHK cells [31] but unlike the multi-modal distributions obtained from a number of in vitro preparations of other types of IF [29,32–34]. The significance of this discrepancy is discussed further below. The measured mean mass-per-unit-length of hard α-keratin IF was 31.2 kDa nm^{-1} and the standard deviation of the measurements was 3.0 kDa nm^{-1}. Knowing that the repeat length in an α-kera-

Fig. 3. Dark-field scanning transmission electron micrograph of unstained, frozen-dried specimens of hard α-keratin filaments isolated from rat vibrissae. The denser straight rods are tobacco mosaic virions, included as mass standards. Bar = 50 nm.

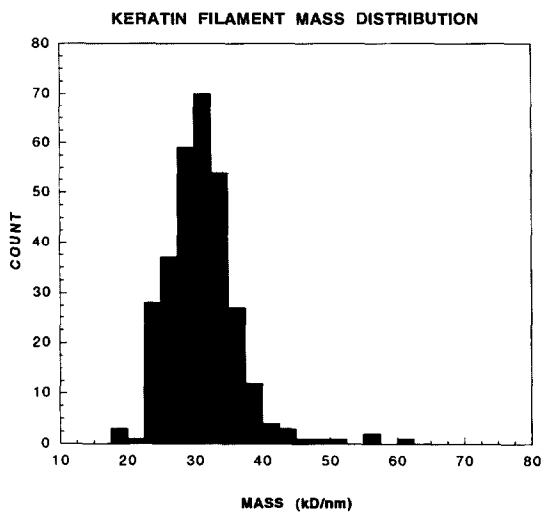

Fig. 4. Distribution of mass-per-unit-lengths determined using STEM for isolated hard α-keratin IF. The mean occurs at 31.2 kDa nm^{-1} (standard deviation 3 kDa nm^{-1}, 305 values) and corresponds to about 30 chains in section.

tin IF is 47.0 nm [24,25] it follows that the total mass per repeat is 31.2×47 kDa i.e. 1466.4 kDa. Each α-keratin molecule is a heterodimer containing a Type I and a Type II chain. Thus for an 8c-1 (Type I) and a 7c (Type II) heterodimer with chain weights 46.66 and 53.57 kDa respectively, the molecule will have a mass of 100.23 kDa. The number of molecules in cross-section is then given by 1466.4/100.23 i.e. 14.63. In round figures, therefore, there are about 15 molecules (30 chains) in a cross-section in a hard α-keratin IF.

To date, it has been possible to study only two kinds of native intermediate filaments by STEM measurements of mass-per-unit-length, i.e. desmin/vimentin copolymers [31] and hard α-keratin (this study). In both cases the preparations were found to be essentially homogeneous, consisting of filaments that contain about 32 chains in cross-section. However, a variety of intermediate filaments that were reassembled in vitro from purified proteins have also been studied in this way [19,29,31–35]. In each case the reassembled filaments were found to be heterogeneous, having several subpopulations with distinct values of mass-per-unit-length. One of these subpopulations matches that of the native filaments, but the others are either more or less dense. These observations indicate that the reassembly reactions were only partially successful in reproducing native filament structure. The data obtained by Kooijman [36] for vimentin IF using the alternative technique of transient electric birefringence are consistent with the proposition that only reassembled IF are polymorphic.

The various density types observed appear to be related by quantized polymorphism, in that each density is an integral multiple of some basic value [35]. Interpretation of distributions of mass-per-unit-length measurements is complicated by the consideration that different polymorphs sometimes merge continuously in the same filament, introducing the risk that a measurement made in a transition zone will yield an average value typical of neither polymorph. Nevertheless, the most plausible interpretation of the cumulative data to date is that the native filaments correspond to a multiple of four, while other polymorphs correspond to multiples of two (about 16 chains), three (about 24 chains) or five (about 40 chains), respectively. These and other data have contributed to the proposal that the basic density unit is a filamentous sub-component, the protofibril [37].

2.4. Surface lattice structure

Crosslinks have been induced in K1/K10 [16] and K5/K14 epidermal keratins [17] (Fig. 5) and vimentin IF [18] using the disulfosuccinimydyl tartrate (DST) reaction. Subsequent chemical characterisation of these crosslinks has allowed the lengths of the links L1, L12 and L2 to be determined, together with the relative axial staggers between the coiled-coil segments (A_{11}, A_{22}, A_{12}) (Fig. 6). In the case of hard α-keratin the large number of disulfide bonds present has precluded a similar approach being taken. Nonetheless it has proved possible to assess these parameters using a rather more indirect means [38]. Firstly, the known surface lattice structure of hard α-keratin as determined from X-ray diffraction methods [24,25] has allowed values of z_a and z_b to be determined i.e. the axial projections of the vectors a and b that specify the surface lattice. From these

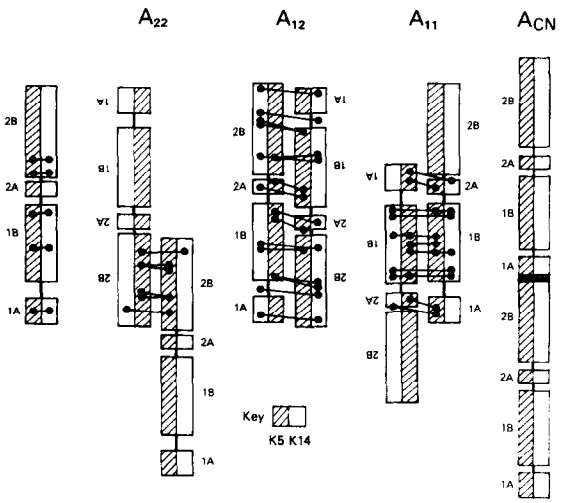

Fig. 5. Lysine–lysine crosslinks were induced between the K5 and K14 chains of human epidermal keratin through the use of the disulfosuccinimidyl tartrate (DST) reaction. Those links show that (a) the two chains constituting the molecule are parallel and in axial register, (b) antiparallel 2B segments largely overlap (A_{22} mode of interaction), (c) antiparallel molecules largely overlap (A_{12} interaction) (d) antiparallel 1B segments largely overlap (A_{11} interaction). In contrast, (e) the A_{CN} mode, is deduced from A_{11} and A_{22}. The axially projected lengths of the links and the values of A_{11}, A_{22} and A_{12} can be determined by a least square analysis knowing the positions of the lysine residues in the two molecules that interact with one another. Reprinted from Steinert et al. [17].

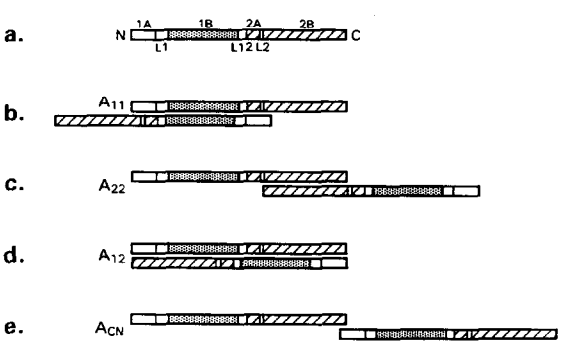

Fig. 6. Summary of the modes of interactions between two epidermal keratin IF molecules. The nomenclature is as given in Fig. 5. The same modes of interaction (except A_{CN}) occur for hard α-keratin though there are significant differences between the precise values of A_{11} and A_{12} in the two cases. In contrast A_{22} is virtually unchanged as are the values of the length of links L1, L12 and L2 (see Table 1).

data two equations can be formulated that relate A_{11}, A_{12} and A_{22}. These are:

$$-2A_{12} + A_{11} + A_{22} = 50.0$$

$$A_{12} - A_{11} = 133.3$$

where the units are in multiples of the residue translation in a coiled-coil (0.1485 nm). Furthermore, the high homology between the amino acid sequences of links L12 and L2 in hard and epidermal α-keratin allows the reasonable assumption that these structures are the same and their axial extent is identical. It follows that

$$L12 = 13.94$$

$$L2 = 5.06$$

A final constraint is derived from the work of Sparrow et al. [11], who showed that the action of chymotrypsin B on hard α-keratin resulted in a transpeptidation event that covalently linked 1B segments from different (antiparallel) molecules. This gives the relationship

$$A_{11} - 0.1L1 + L12 + L2 = -109$$

We thus have five equations relating six parameters (L1, L12, L2, A_{11}, A_{22}, A_{12}). At least one further constraint is required before a solution can be found. Other data [13,14] showed that a highly favoured stagger between antiparallel 1B segments was -5 or -16 residues. The former gives rise to the unlikely situation in which link L1 is exceptionally short whereas the second value yields a physically reasonable structure similar to that previously determined for the epidermal keratins. Hence, solving the six equations leads to a model for hard α-keratin compatible with all of the (limited) data currently available [21] (Table 2). Values of the structural parameters determined for epidermal keratin and vimentin have also been listed in Table 1 for comparison with those for α-keratin. It is immediately apparent that many of the parameters for α-keratin and epidermal keratin are very similar (A_{22}, L1, Δz(2BU, 2BD)) as are those for hard α-keratin and vimentin (z_b, overlap, A_{12}, A_{11}, Δz(1BU,2D), Δz(1BU,1BD)). (The nomenclature Δz(1BU,1BD), for instance, refers to the relative axial stagger in the z-direction between up-pointing (U) and down-pointing (D) 1B segments). It would seem that α-keratin can, in many respects, be considered as a hybrid of the epidermal keratin and vimentin structures.

Table 1
Axial parameters for the model of hard α-keratin, and a comparison with those derived experimentally for epidermal keratin and vimentin IF

	α-Keratin	K1/5/10/14	Vimentin
z_A	50.0	80.34	26.43
z_B	**133.3**	112.05	**130.60**
Repeat	316.6	304.44	287.63
Overlap	−9.09	**6.83**	**8.09**
A_{12}	6.38	**0.43**	**−0.45**
A_{11}	**−126.92**	−111.62	**−131.05**
A_{22}	**189.68**	**192.82**	156.58
L1	**12.51**	**16.27**	5.24
L12	**13.94**	**13.94**	6.06
L2	**5.06**	**5.06**	8.41
Δz(1BU,1BD)	**−15.43**	−3.89	**−16.81**
Δz(2BU,2BD)	**3.17**	**2.56**	−18.14
Δz(1BU,2D)	**−41.13**	−50.84	**−40.69**

Each of these values represents a distance corresponding to the equivalent number of residues in a coiled-coil conformation. Thus the physical magnitudes are determined by multiplying each value by 0.1485 nm. Pairs of bold values indicate the similarity between the parameters derived for hard α-keratin, epidermal keratin (K1/5/10/14) and vimentin. In many respects α-keratin is a hybrid of the structures determined experimentally for epidermal keratin and vimentin.

One difference that is particularly important, however, is that the characteristic and common overlap between parallel molecules in vimentin and in epidermal keratin (about 7–8 residues) is absent in hard α-keratin. Indeed, the results show that there is a gap of about nine residues between the ends of the rod domains of parallel molecules. Since mutations in the overlap region are known to be related to the incidence of keratinopathies [1], presumably through compromising its stabilising role in the molecular assembly process, its absence in hard α-keratin was unexpected, especially so since the amino acid sequences involved in the overlap region were conserved in large part. In Section 2.5 however, it will be shown that a compensating network of disulfide bonds is possible.

2.5. Disulfide bond network

The model structure proposed for hard α-keratin results in many of the cysteine residues in neighbouring molecules being axially aligned in the topological surface lattice structure, thus giving rise to the potential of a network of intermolecular disulfide bonds. Although the cysteine residues are calculated to lie axially within ±2 residues of one another there is no evidence that these residues are appropriately positioned azimuthally. This would be required if disulfide bond formation is to occur. No direct chemical characterisation of a disulfide bond in hard α-keratin has yet been demonstrated but it is commonly believed that such covalent links are probable. Certainly it has been reported that 97–98% of cysteine residues in hard α-keratin occur in vivo in the cystine form [39], so it is certain that some at least (and probably most) of the cysteine residues in the IF proteins do form disulfide links with either other IF proteins or other subunits of the matrix.

A hard α-keratin heterodimer consisting of an 8c-1 and a 7c chain contains 17 cysteine residues within the rod domain. The positions of the cysteine residues immediately following the C-terminal end of segment 2B can also be specified axially since the lengths of the coiled-coil segments and the links have all been determined (see Table 1). Knowing the surface lattice of hard α-keratin IF [24,25] it is possible to write down the relative positions of the cysteine residues in the four molecules thought to constitute the structural 'unit'. The coordinates are as follows: $z_0 = z$; $z_1 = 314.89 - z$; $z_2 = z + 133.30$; $z_3 = 314.89 - z + 133.30$; $z_4 = z - 50.0$, where z values are those calculated from the basic molecule (Table 2). Parry [21] showed that potential disulfide bonds could be formed as follows: 1B-17 with 2B-63, C-1 with 1A-6, 2B-88 with L1-5, L1-9 with 1B-87, 1B-17 with 1B-70, 2B-63 with 2B-63, 2B-22 with 2B-105 and 2B-5 with 2B-119 for molecules one apart [21]; 1B-17 with 2B-63, L1-9 with 2B-45 and 1B-70 with 2B-63 for molecules two apart; 2B-70 with 2B-5 for molecules three apart; 1A-6 with 2B-88, 2B-119 with 2B-70, 2B-70 with 2B-22, 2A-4 with 1B-70 and 1B-66 with 1B-17 for molecules four apart on the topological surface lattice [38]. Note that separation on the topological surface lattice does not imply spatial separation in the IF itself. If the disposition of disulfide bonds was a cyclic one then it follows that a subfibrillar structure such as a protofibril (containing eight chains, for example) might be present, in line with the indications of such an entity derived from the STEM data. It remains a matter of speculation at this stage that the disulfide bonds do define such a structure.

2.6. Low-angle X-ray diffraction pattern

Fraser and MacRae [20] interpreted the low-angle X-ray diffraction pattern of hard α-keratin in terms of an array of solid cylinders with radii of about 3.65 nm. From a calculation of the excluded volume of a keratin heterodimer and the volume of a repeat of an hard α-keratin IF it appeared that there could be only about 23 molecules in cross-section [38]. This value is clearly different from that derived from the STEM data presented in Section 2.3. In addition, other evidence derived from the structure of β-keratin indicated about 26 chains in section [22].

An analysis of the X-ray diffraction data has shown that an alternative family of models for the IF is indeed compatible with the experimental observations. Suppose that the IF is considered as a cylinder with a core substructure (Fig. 7). In negatively stained preparations of isolated hard α-keratin IF examined by transmission electron microscopy evidence for a core substructure has been demonstrated [2]. The core may have a density less than or greater than that of the cylinder in which it occurs, depending on whether the value of ρ_2 is negative or positive (Fig. 7). The value of the outer and inner radii, as well as their electron densities, are parameters that can be varied to fit the following constraints; the diameter of the IF must be large enough to accommodate 32 chains (say) and the positions of the observed equatorial diffraction maxima at spacings of 4.5 and 2.7 nm must agree with those predicted from the model (and hence be consistent with that calculated for a

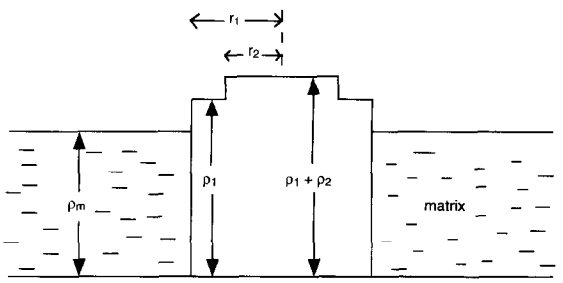

Fig. 7. Model of a hard α-keratin IF embedded within a matrix of density ρ_m. The radius of the IF is r_1 and that of the core is r_2. The densities of the core and the peripheral region of the IF are $\rho_1 + \rho_2$ and ρ_1 respectively. Note that ρ_2 may be positive or negative, thus generating either a structure with a dense core and a less dense periphery, or a structure that is essentially annular in form.

Table 2
Axial disposition of potential disulphide bonds in a hard α-keratin IF

Molecule 0		Molecule 1		Molecule 2		Molecule 3		Molecule 4	
z_0	residue	z_1	residue	z_2	residue	z_3	residue	z_4	residue
309.51	C-2	308.89	1A-6	299.75	2A-4	313.68	1B-87	312.66	L1-9
308.51	C-1	273.75	L1-5	267.81	1B-87	281.74	2A-4	308.97	L1-6
305.51	2B-119	272.52	L1-6	250.81	1B-70	256.68	2B-5	307.74	L1-5
291.51	2B-105	268.83	L1-9	246.81	1B-66	239.68	2B-22	272.6	1A-6
274.51	2B-88	250.38	1B-17	197.81	1B-17	216.68	2B-45	259.51	C-2
256.51	2B-70	201.38	1B-66	179.36	L1-9	198.68	2B-63	258.51	C-1
249.51	2B-63	197.38	1B-70	175.67	L1-6	191.68	2B-70	255.51	2B-119
231.51	2B-45	180.38	1B-87	174.44	L1-5	173.68	2B-88	241.51	2B-105
208.51	2B-22	148.44	2A-4	139.3	1A-6	156.68	2B-105	224.51	2B-88
191.51	2B-5	123.38	2B-5	126.21	C-2	142.68	2B-119	206.51	2B-70
166.45	2A-4	106.38	2B-22	125.21	C-1	139.68	C-1	199.51	2B-63
134.51	1B-87	83.38	2B-45	122.21	2B-119	138.68	C-2	181.51	2B-45
117.51	1B-70	65.38	2B-63	108.21	2B-105	125.59	1A-6	158.51	2B-22
113.51	1B-66	58.38	2B-70	91.21	2B-88	90.45	L1-5	141.51	2B-5
64.51	1B-17	40.38	2B-88	73.21	2B-70	89.22	L1-6	116.45	2A-4
46.06	L1-9	23.38	2B-105	66.21	2B-63	85.53	L1-9	84.51	1B-87
42.37	L1-6	9.38	2B-119	48.21	2B-45	67.08	1B-17	67.51	1B-70
41.14	L1-5	6.38	C-1	25.21	2B-22	18.08	1B-66	63.51	1B-66
6.00	1A-6	5.38	C-2	8.21	2B-5	14.08	1B-70	14.51	1B-17

Each of these values represents an axial coordinate equivalent to the number of residues in a coiled-coil conformation. Physical magnitudes can be determined by multiplying each value by 0.1485 nm.

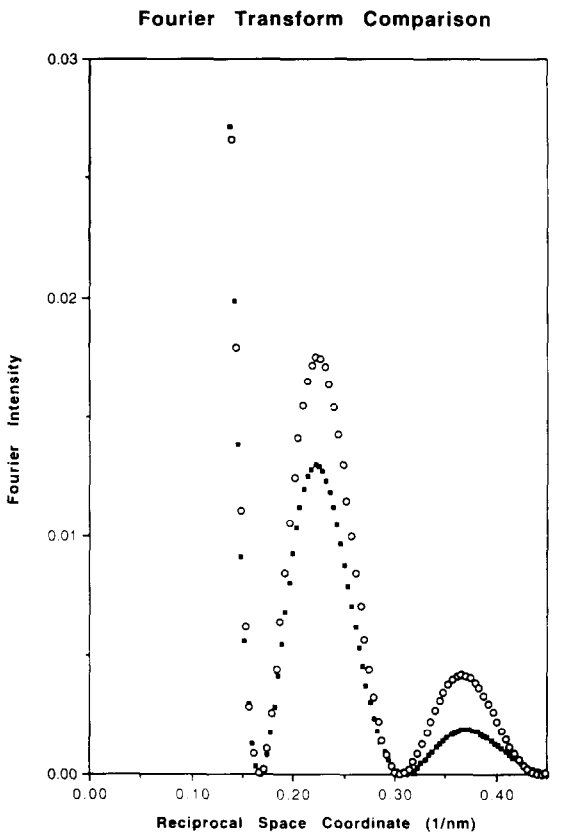

Fig. 8. Normalised Fourier transform (circles) of a solid cylinder of radius 3.65 nm compared to that from a cylinder of outer radius 4.39 nm with a core of radius 3.47 nm (filled squares). The peaks in the low-angle region of the X-ray diffraction pattern are in the same position, illustrating that the pattern can be interpreted in terms of different structures (i.e. with different radii and electron density distributions).

solid, uniformly dense cylinder). A number of solutions are compatible with the data (Fig. 8), two of which were detailed by Parry [38]. The important point is that there are indeed models for the IF in section that are compatible with the equatorial X-ray data and which can contain 32 chains. In this respect, therefore, there is no longer any need for concern about what was an apparent discrepancy between the STEM and X-ray data.

In the case of the β-keratin data the number of chains in a β-crystallite was calculated as 26. This was made up of the refined values for the number of chains per sheet (10.1) and the number of sheets (2.6) in the β-crystallite. Physically it is not easy to understand how a non-integral value for the number of sheets could arise, and a value of three rather than 2.6 seems more probable. If this was the case then the β-keratin data would also predict 30 chains, a value in close agreement with the other estimates.

3. Conclusion

Taken together with the results of many earlier studies, the current work supports the following working hypothesis. Native intermediate filaments —at least those of hard α-keratin and vimentin— have uniquely defined and closely similar structures with, on average, about 32 chains in cross-section. This structure is at least partially reproduced in the in vitro assembly systems that have been studied, although polymorphic variants containing differing numbers of protofibrils (16, 24 or 40 chains) are also common assembly products. It seems likely that native epidermal keratin and vimentin homopolymer IF and, most likely, many other kinds of native IF as well will also prove to be 32-chain structures. This model may well apply more widely to other kinds of keratin IF and other IF generally [1], although this proposition has yet to be addressed experimentally.

A second provisional conclusion is that hard α-keratin IF appear to differ from other IF in lacking the head-to-tail overlap between parallel molecules packed in the filament, an arrangement that is thought to lend stability. This discrepancy primarily reflects a difference between the respective axial repeats, which are thought to be longer in hard α-keratin (47 nm), as deduced from indexation of X-ray fibre diffraction patterns [24,25], than in epidermal keratin or vimentin (about 45.2 and 42.7 nm respectively) as deduced from the chemical cross-linking data [16–18]. Bearing in mind the highly conserved nature of the amino acid sequences that comprise this overlap region, including those in hard α-keratin, it was surprising that the data did not support a common model. In hard α-keratin, however, the cysteine residues are in an axial position that would allow the formation of disulfide bonds with other IF molecules.

If so, then stabilisation is probably achieved far more effectively than through a head-to-tail molecular overlap seen for those classes of IF which, in essence, lack cysteine residues in their rod domains.

It can be concluded that there are at least four unique IF structures as judged by their different axial repeats. Nonetheless, it would seem that all IF probably contain the same number of chains in section, and that four protofibrils constitute the basic IF structure. The molecules aggregate through the same fundamental axial alignments (A_{11}, A_{22}, A_{12}) though the precise values of these alignments differ from one type of IF to another, thus generating the observed (different) axial repeats. Intermediate filaments thus provide a delightful mix of conserved and variable elements, designed in part to prevent inappropriate molecular aggregation and, presumably, in part to allow functioning in the most effective manner.

Acknowledgements

One of us (LNJ) is indebted to the International Wool Secretariat and the Cooperative Research Centre for Premium Quality Wool for support in undertaking this project. We also thank Drs Naiqian Cheng and James Conway for making available electron microscopy and computing resources used in this study; Drs Joe Wall, Jim Hainfeld and their colleagues for support at the Brookhaven STEM Facility; Dr S. Cushman, (NIDDK), for kind provision of experimental materials.

References

[1] D.A.D. Parry, P.M. Steinert, Intermediate Filament Structure, Springer-Verlag, Heidelberg, 1995.
[2] L.N. Jones, Biochim. Biophys. Acta 446 (1976) 515–524.
[3] R.D.B. Fraser, T.P. MacRae, G.E. Rogers, Keratins: Their Composition, Structure and Biosynthesis, Charles C. Thomas, Springfield, Il, 1972.
[4] J.M. Gillespie, in: R.D. Goldman, P.M. Steinert (Eds.), Cellular and Molecular Biology of Intermediate Filaments, Plenum, New York, 1990, pp. 95–128.
[5] L.N. Jones, I.J. Kaplin, G.J.F. Legge, J. Computer-Assisted Microsc. 5 (1993) 85–89.
[6] W.G. Crewther, L.M. Dowling, K.H. Gough, R.C. Marshall, L.G. Sparrow, in: D.A.D. Parry, L.K. Creamer (Eds.), Fibrous Proteins: Scientific, Industrial and Medical Aspects, Academic Press, London, 1980, pp. 151–159.
[7] C. Cohen, D.A.D. Parry, Proteins-Struct. Funct. Genet. 7 (1990) 1–15.
[8] J.H. Brown, C. Cohen, D.A.D. Parry, Proteins: Structure, Function and Genetics 26 (1997) 134–145.
[9] D.A.D. Parry, W.G. Crewther, R.D.B. Fraser, T.P. MacRae, J. Mol. Biol. 113 (1977) 449–454.
[10] E.F. Woods, A.S Inglis, Int. J. Biol. Macromol. 6 (1984) 277–283.
[11] L.G. Sparrow, L.M. Dowling, V.Y. Loke, P.M. Strike, in: G.E. Rogers, P.J. Reis, K.A. Ward, R.C. Marshall (Eds.), The Biology of Wool and Hair, Chapman and Hall, London, 1989, pp. 145–155.
[12] A.D. MacLachlan, M. Stewart, J. Mol. Biol. 162 (1982) 693–698.
[13] R.D.B. Fraser, T.P. MacRae, E. Suzuki, D.A.D. Parry, Int. J. Biol. Macromol. 7 (1985) 258–274.
[14] R.D.B. Fraser, T.P. MacRae, D.A.D. Parry, E. Suzuki, Proc. Natl. Acad. Sci. USA 83 (1986) 1179–1183.
[15] W.G. Crewther, L.M. Dowling, P.M. Steinert, D.A.D. Parry, Int. J. Biol. Macromol. 5 (1983) 267–274.
[16] P.M. Steinert, L.N. Marekov, R.D.B. Fraser, D.A.D. Parry, J. Mol. Biol. 230 (1993) 436–452.
[17] P.M. Steinert, L.N. Marekov, D.A.D. Parry, Biochemistry 32 (1993) 10046–10056.
[18] P.M. Steinert, L.N. Marekov, D.A.D. Parry, J. Biol. Chem. 268 (1993) 24916–24925.
[19] S. Heins, P.C. Wong, S. Muller, K. Goldie, D.W. Cleveland, U. Aebi, J. Cell Biol. 123 (1993) 1517–1533.
[20] R.D.B. Fraser, T.P. MacRae, Biochim. Biophys. Acta 29 (1958) 229–240.
[21] D.A.D. Parry, Proteins: Struct. Funct. Genet. 22 (1995) 267–272.
[22] R.D.B. Fraser, T.P. MacRae, D.A.D. Parry, E. Suzuki, Polymer 10 (1969) 810–826.
[23] D. Thomas, P. Schultz, A.C. Steven, J.S. Wall, Biol. Cell 80 (1994) 181–192.
[24] R.D.B. Fraser, T.P. MacRae, Biosci. Rep. 3 (1983) 517–525.
[25] R.D.B. Fraser, T.P. MacRae, Biosci. Rep. 5 (1985) 573–579.
[26] L.N. Jones, F.M. Pope, J. Cell Biol. 101 (1985) 1569–1577.
[27] M.W. Mosesson, J.F. Hainfeld, J.S. Wall, R.H. Haschemeyer, J. Mol. Biol. 153 (1981) 695–718.
[28] J.S. Wall, J.F. Hainfeld, Ann. Rev. Biophys. Biophys. Chem. 15 (1986) 355–376.
[29] A.C. Steven, J.F. Hainfeld, B.L. Trus, J.S. Wall, P.M. Steinert, J. Cell Biol. 97 (1983) 1939–1944.
[30] B.L. Trus, E. Kocsis, J.F. Conway, A.C. Steven, J. Struct. Biol. 116 (1996) 61–67.
[31] A.C. Steven, J.S. Wall, J.F. Hainfeld, P.M. Steinert, Proc. Natl. Acad. Sci. USA 79 (1982) 3101–3105.
[32] S. Heins, U. Aebi, Curr. Opin. Cell Biol. 6 (1994) 25–33.
[33] A. Engel, R. Eichner, U. Aebi, J. Ultrastruct. Res. 90 (1985) 323–335.

[34] A.C. Steven, J.F. Hainfeld, B.L. Trus, J.S. Wall, P.M. Steinert, J. Biol. Chem. 258 (1983) 8323–8329.
[35] A.C. Steven, in: R.D. Goldman, P.M. Steinert (Eds.), Cellular and Molecular Biology of Intermediate Filaments, Plenum Press, New York, 1994, pp. 233–263.
[36] M. Kooijman, Ph.D. Thesis, Vrije University of Amsterdam (1995).
[37] U. Aebi, W.E. Fowler, P. Rew, T.-T. Sun, J. Cell Biol. 97 (1983) 1131–1143.
[38] D.A.D. Parry, Int. J. Biol. Macromol. 19 (1996) 45–50.
[39] R.D.B. Fraser, T.P. MacRae, L.G. Sparrow, D.A.D. Parry, Int. J. Biol. Macromol. 10 (1988) 106–112.